Received: 3 February 2023 | Revised: 26 April 2023 | Accepted: 5 May 2023

DOI: 10.1111/cas.15853

ORIGINAL ARTICLE

Cancer Science WILEY

# Relationships between physical and immunological tumor microenvironment in pancreatic ductal adenocarcinoma

Yu Igata[1,2] | Motohiro Kojima[3] | Toshiyuki Suzuki[4] | Genichiro Ishii[5] | Ryo Morisue[1,3] | Toshihiro Suzuki[6,7] | Masashi Kudo[1] | Motokazu Sugimoto[1] | Shin Kobayashi[1] | John D. Martin[8] | Triantafyllos Stylianopoulos[9] | Horacio Cabral[10] | Mitsunobu R. Kano[11] | Masaru Konishi[1] | Naoto Gotohda[1,2]

[1]Department of Hepatobiliary and Pancreatic Surgery, National Cancer Center Hospital East, Kashiwa, Japan

[2]Course of Advanced Clinical Research of Cancer, Juntendo University Graduate School of Medicine, Tokyo, Japan

[3]Division of Pathology, Exploratory Oncology Research and Clinical Trial Center, National Cancer Center, Kashiwa, Japan

[4]Department of Surgery, Hanyu General Hospital, Hanyu, Japan

[5]Department of Pathology and Clinical Laboratories, National Cancer Center Hospital East, Kashiwa, Japan

[6]Division of Pharmacology, School of Medicine, Teikyo University, Tokyo, Japan

[7]Department of Cancer Immunotherapy, Exploratory Oncology Research and Clinical Trial Center, National Cancer Center, Kashiwa, Japan

[8]Red Arrow Therapeutics Co., Ltd, Tokyo, Japan

[9]Cancer Biophysics Laboratory, Department of Mechanical and Manufacturing Engineering, University of Cyprus, Nicosia, Cyprus

[10]Department of Bioengineering, Graduate School of Engineering, The University of Tokyo, Tokyo, Japan

[11]Department of Pharmaceutical Biomedicine, Graduate School of Interdisciplinary Science and Engineering in Health Systems, Okayama University, Okayama, Japan

**Correspondence**
Motohiro Kojima, Division of Pathology, Exploratory Oncology Research and Clinical Trial Center, National Cancer Center, 6-5-1 Kashiwanoha, Kashiwa, Chiba 277-8577, Japan.
Email: mokojima@east.ncc.go.jp

**Funding information**
Fund for the Promotion of Joint International Research, Grant/Award Number: 21K

## Abstract

Pancreatic ductal adenocarcinoma (PDAC) is physically palpated as a hard tumor with an unfavorable prognosis. Assessing physical features and their association with pathological features could help to elucidate the mechanism of physical abnormalities in cancer tissues. A total of 93 patients who underwent radical surgery for pancreatic and bile duct cancers at a single center hospital during a 28-month period were recruited for this study that aimed to estimate the stiffness of PDAC tissues compared to the other neoplasms and assess relationships between tumor stiffness and pathological features. Physical alterations and pathological features of PDAC, with or without preoperative therapy, were analyzed. The immunological tumor microenvironment was evaluated using multiplexed fluorescent immunohistochemistry. The stiffness of PDAC correlated with the ratio of Azan-Mallory staining, α-smooth muscle actin, and collagen I-positive areas of the tumors. Densities of $CD8^+$ T cells and $CD204^+$ macrophages were associated with tumor stiffness in cases without preoperative therapy. Pancreatic ductal adenocarcinoma treated with preoperative therapy

**Abbreviations:** αSMA, α-smooth muscle actin; ART, area of residual tumor; BDC, bile duct cancer; FFPE, formalin-fixed, paraffin-embedded; HABP, hyaluronan-binding protein; IPMN, intraductal papillary mucinous neoplasm; PDAC, pancreatic ductal adenocarcinoma; S-1, tegafur/gimeracil/oteracil; TME, tumor microenvironment.

was softer than that without, and the association between tumor stiffness and immune cell infiltration was not shown after preoperative therapy. We observed the relationship between tumor stiffness and immunological features in human PDAC for the first time. Immune cell densities in the tumor center were smaller in hard tumors than in soft tumors without preoperative therapies. Preoperative therapy could alter physical and immunological aspects, warranting further study. Understanding of the correlations between physical and immunological aspects could lead to the development of new therapies.

**KEYWORDS**
elasticity, immunology, pancreatic neoplasm, pathology, tumor microenvironment

## 1 | INTRODUCTION

Pancreatic ductal adenocarcinoma is an aggressive malignancy with the highest mortality rate among solid tumors. It is also known to be a hard mass, and its representative pathology of the prominent stromal component seems to be associated with this physical feature and aggressive clinical behavior.[1] Furthermore, increased stiffness in PDAC has been shown to induce invasion and metastasis of cancer cells[2] and acts as a barrier to anticancer drugs, including immune checkpoint inhibitors.[3,4] Recently, this physical aspect of the TME has been reported to play pivotal roles in tumor initiation, progression, and resistance to cancer treatment.[5] To this end, the close relationship between tumor pathophysiology and the physical aspects of cancer has led to the development of novel cancer treatment strategies.[6] These strategies involve remedies to normalize the abnormal physical TME, which has already been explored in murine tumor models showing synergistic effects with conventional treatments, and is leading to the discovery of combining agents to normalize the TME at the bedside.[7–9] However, knowledge about how the physical characteristics of human tumors are related to pathological features is still largely limited; therefore, the clinical application of these theories based on mouse models to human tumors has remained limited.

In this study, we evaluated the stiffness of PDAC, IPMN, and BDC using a tonometer to investigate organ- and histology-dependent physical features in human tumors. Next, focusing on PDAC, we analyzed the association between tumor stiffness and pathological features using multiplex fluorescent immunohistochemistry. Finally, tumor stiffness and pathological features were compared between patients with and without preoperative therapy to evaluate the histological and physical alterations in the TME due to preoperative therapy in PDAC.

## 2 | METHODS

### 2.1 | Study cohorts

A total of 93 patients who underwent radical surgery for select neoplasms at the Department of Hepatobiliary and Pancreatic Surgery, National Cancer Center Hospital East, between June 2018 and September 2020, were enrolled in this study. These included patients with PDAC (58), IPMN (18), and BDC (17), and the operative procedures were pancreaticoduodenectomy (64), distal pancreatectomy (25), and total pancreatectomy (4). Of the 58 patients with PDAC, 35 had preoperative therapy. The regimens of the preoperative therapy were gemcitabine and S-1 in 19 patients, gemcitabine and nab-paclitaxel in 13, and S-1 and radiation in 3. Clinical data were extracted from the medical records. During this period, the surgical procedure was standardized, and the treatment decision with or without preoperative therapy was selected based on a multidisciplinary team conference. This study was approved by the institutional review board of the National Cancer Center (IRB number: 2012-067).

### 2.2 | Stiffness estimated by measurement of displacement of tissues

We estimated the stiffness of the resected tissues using a tonometer, iB-Dent (Koganei; Figure 1). The iB-Dent measures the displacement of the tissue after applying an air pressure of 100 kPa at the micrometer level, and thus a larger displacement is seen in softer tissues. We previously reported a method for measurement of the stiffness of colorectal and pancreatic tissues using the Venustron system (Axiom), which is an automatic indentation apparatus.[10,11] In the current study, using standardized silicone materials, we confirmed that the stiffness estimated by the iB-Dent correlated strongly with the measurement by the Venustron system, which supports the reliability of the stiffness estimation in this study (Figure S1).

After the pancreas was resected, we determined the location of the tumor by palpation, and then we cut vertically to confirm the precise location of the tumor. For BDC, the posterior wall of the bile duct was cut longitudinally, allowing direct macroscopic detection of the tumor. Displacement was measured from the anterior surface for pancreatic tumors and directly for BDC. Five random points of the tumor and the normal tissues were selected for the measurements, and the mean values of the five measurements were used for the analysis. The displacement of normal pancreatic tissue was measured at the pancreatic stump in the same manner. Finally, the

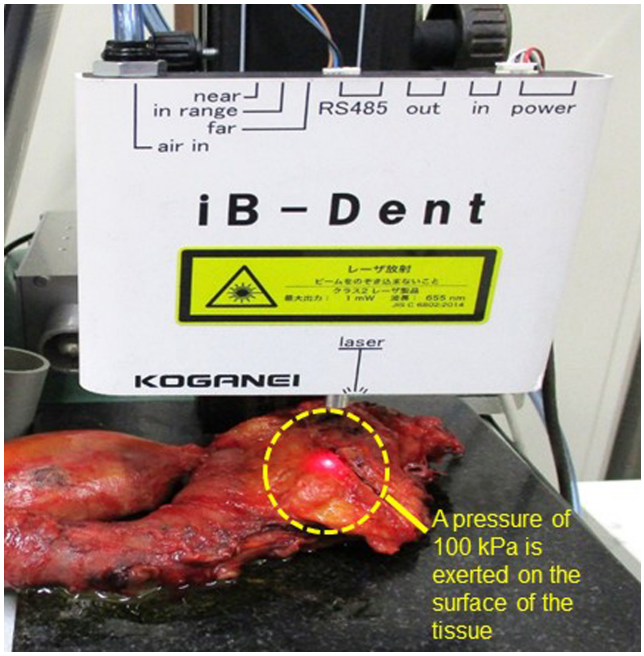


**FIGURE 1** Measurement of displacement of pancreatic ductal adenocarcinoma after surgery using iB-Dent. A pressure of 100 kPa is exerted on the surface of the tissue and the resulting displacement is measured. Stiffer tissues deform (displace) less than softer tissues.

presence of tumor tissue at the measurement site was microscopically confirmed by H&E staining of FFPE sections.

## 2.3 | Histological evaluation

The UICC TNM Classification System (8th edition) was used for pathological diagnosis. The FFPE specimens obtained from patients with pancreatic cancer were cut into 3-μm-thick serial sections. The sections were stained by Azan–Mallory stain (Azan) for collagen fiber staining. Immunohistochemical staining for αSMA and collagen I was carried out automatically using the Ventana Benchmark ULTRA (Ventana Medical Systems). Monoclonal anti-human αSMA Ab (Clone:1A4; Dako) and anti-human collagen I Ab (Clone:3G3, RayBiotech) were used at a dilution of 1:100, and the conditions for antigen retrieval and primary Ab incubation were set to 91°C for 8 min and 35°C for 60 min, respectively. Biotinylated recombinant HABP (Hokudo) with and without hyaluronidase treatment was used to detect hyaluronic acid. The slides were photographed using a NanoZoomer Digital Pathology Virtual Slide Viewer (Hamamatsu Photonics) and subjected to morphometric analysis using methods previously described.[10,11] For the evaluation of Azan-positive collagen fibers and immunohistochemical αSMA, collagen I expression, and histochemistry of HABP with and without hyaluronidase treatment, ×40 magnification images were taken and saved as JPEG files. The ratio of positive areas in the JPEG files was calculated using morphometric software with color-detecting algorithms (WinROOF software, version 6.5; Mitani Corporation). To assess hyaluronic acid, biotinylated HABP-positive areas without hyaluronidase treatment were subtracted from those with hyaluronidase treatment. Presence of histological tumor necrosis, as previously reported, was also analyzed.[12]

## 2.4 | Multiplexed fluorescent immunohistochemistry for assessment of immunological TME

Serial sections (3 μm thick) were obtained from each FFPE tumor specimen and subjected to multiplexed fluorescent immunohistochemistry using the Opal IHC kit (PerkinElmer), as previously reported.[13,14] The following primary Abs were used: anti-human CD3 (Clone: SP7, 1:600; Abcam), anti-human CD4 (Clone: 4B12, 1:200; Novocastra), anti-human CD8 (Clone: 4B11, 1:160; Novocastra), anti-human CD68 (Clone: M0876, 1:12,000; Dako), anti-human CD204 (Clone: SRA-E5, 1:200; TransGenic Inc.), and cytokeratin (Clone: IR053, 1:100, Dako). Spectral DAPI (PerkinElmer) was used to stain nuclei. Multiplexed fluorescently labeled images (669 × 500 μm each) of the tumor periphery (20 fields) and center (six fields) were captured using an automated imaging system (Vectra version 3.0; PerkinElmer). Image analysis software (InForm; PerkinElmer) was used to determine each cell by its nuclei and to detect immune cells with specific phenotypes.

Tissue segmentation and phenotype recognition were repeated until the algorithm reached the confidence level recommended by the program supplier (at least 90% accuracy) before performing the evaluation. Infiltrating immune cells were quantified using an analytic software program (Spotfire; Tibco) and then calculated per unit area. Using Spotfire, the $CD3^+$ population in $CD4^+$ and $CD8^+$ cells and the $CD204^+$ population in $CD68^+$ macrophages were divided according to the fluorescence signal intensity.

## 2.5 | Measurement of ART

Area of residual tumor was measured to assess the relationship between tumor stiffness and therapeutic effect, using methods previously reported.[15,16] In cases of preoperative therapy, H&E stained slides from the maximum diameter of the tumor were digitally scanned and used for morphometric analysis. Viable residual tumor areas were outlined and calculated using the NanoZoomer Digital Pathology Virtual Slide Viewer (Hamamatsu Photonics, scanned by a ×40 ocular lens). In situ lesions and acellular mucous lakes were excluded from measurements in this study. All tumor nests greater than 0.1 $mm^2$ were measured for ART. Isolated viable tumor foci >2 mm from the largest tumor area on the slide were also identified and calculated individually. The sum of the tumor areas was defined as the ART (Figure S2).

## 2.6 | Statistical analysis

Comparisons between groups were undertaken using the Mann–Whitney *U*-test and Fisher's exact test. The correlation between the

stiffness and morphometric analysis and ART was evaluated using Spearman's correlation coefficient ($\rho$). All calculated $p$ values were two-sided, and $p<0.05$ was considered statistically significant. For prognostic analysis, early tumor recurrence was defined as tumor recurrence ≤12 months after tumor removal. All statistical analyses were performed using EZR (Saitama Medical Center, Jichi Medical University), a graphical user interface for R (The R Foundation for Statistical Computing). More precisely, it is a modified version of the R commander designed to add statistical functions frequently used in biostatistics.[17]

## 3 | RESULTS

### 3.1 | Patient characteristics

The clinical features and pathological data information for the full patient cohort ($n=93$) and the PDAC patient cohort ($n=58$) are summarized in Tables 1 and 2, respectively. The median age of the entire cohort was 68 years (range, 44–88 years), with 54 (58.1%) men and 39 (41.9%) women. The full patient cohort comprised 58 (62.4%) patients with PDAC, 18 (19.4%) with IPMN, and 17 (18.3%) with BDC. The operative procedures were pancreaticoduodenectomy in 64 patients (68.8%), distal pancreatectomy in 25 (26.9%), and total pancreatectomy in four patients (4.3%).

Among the patients with PDAC, 35 (60.3%) were treated with preoperative therapy and 23 (39.6%) patients did not receive preoperative therapy (Table 2). Patient age, sex, and tumor size did not differ between patients who did and did not receive preoperative therapy, although the frequency of lymph node metastasis and advanced stages were higher in patients who did not receive preoperative therapy.

**TABLE 1** Characteristics of patients who underwent radical surgery for pancreatic and bile duct cancers ($n=93$)

| Patient characteristics | Total patients ($n=93$) |
|---|---|
| Age, years (range) | 68 (44–88) |
| Male gender (%) | 54 (58.1) |
| Diagnosis | |
| PDAC (%) | 58 (62.4) |
| IPMN (%) | 18 (19.4) |
| BDC (%) | 17 (18.3) |
| Operative procedure | |
| PD (%) | 64 (68.8) |
| DP (%) | 25 (26.9) |
| TP (%) | 4 (4.3) |

Abbreviations: BDC, bile duct cancer; DP, distal pancreatectomy; IPMN, intraductal papillary mucinous neoplasm; PD, pancreaticoduodenectomy; PDAC, pancreatic ductal adenocarcinoma; TP, total pancreatectomy.

**TABLE 2** Characteristics of patients with pancreatic ductal adenocarcinoma (PDAC), with or without preoperative therapy ($n=58$)

| PDAC patient characteristics | Without preoperative therapy ($n=23$) | With preoperative therapy ($n=35$) | $p$ value |
|---|---|---|---|
| Age, years (range) | 68 (44–85) | 68 (46–87) | 0.386 |
| Male gender (%) | 9 (39) | 16 (45) | 0.787 |
| Tumor size, mm (range) | 27 (12–60) | 24 (10–100) | 0.105 |
| Positive lymph node metastasis (%) | 20 (87) | 18 (51) | 0.010 |
| Pathological stage I/II/III/IV | 3/12/7/1 | 17/9/9/0 | 0.029 |
| Displacement, μm (range) | 512.6 (61.2–2564.6) | 906.4 (184.6–2162.0) | 0.006 |
| Azan-positive area, % (range) | 36.7 (8.9–50.1) | 33.9 (15.2–50.1) | 0.188 |
| Collagen I-positive area, % (range) | 43.6 (18.5–58.1) | 36.5 (20.3–57.6) | 0.455 |
| αSMA-positive area, % (range) | 31.1 (13.7–45.2) | 26.9 (14.0–43.4) | 0.164 |
| Hyaluronic acid content, % (range) | 43.0 (0.9–73.3) | 62.6 (0.8–85.1) | 0.005 |

Abbreviation: αSMA, α-smooth muscle actin.

### 3.2 | Variation of stiffness among tumor origins, histological features, and preoperative therapy

We measured the stiffness of PDAC tissues using a tonometer (iB-Dent; Figure 1). According to the mean displacement measured by iB-Dent, PDAC tissue was significantly stiffer than normal pancreatic tissue (796 vs. 1989 μm, $p<0.001$). Pancreatic ductal adenocarcinoma was stiffer compared to IPMN and BDC ($p<0.001$), suggesting a histologically dependent variability (Figure 2). Tumor stiffness in PDAC cases with and without preoperative therapy showed significant differences (906.4 vs. 512.6 μm, $p=0.006$). Pancreatic ductal adenocarcinoma was the stiffest among the tumors tested, as it was approximately threefold stiffer than IPMN and twofold stiffer than BDC.

### 3.3 | Association between tumor stiffness and histological data of stromal components in PDAC

We stained, and automatically segmented with image analysis software, Azan (Figure 3A), αSMA (Figure 3B), collagen I (Figure 3C), and hyaluronic acid in hyaluronidase untreated (Figure 3D) and treated (Figure 3E) tumor tissue sections.

The ratio of the positive area of the hyaluronic acid component of the stroma was greater in PDAC patients who received preoperative therapy than in those who did not (62.6% vs. 43.0%; $p=0.005$).

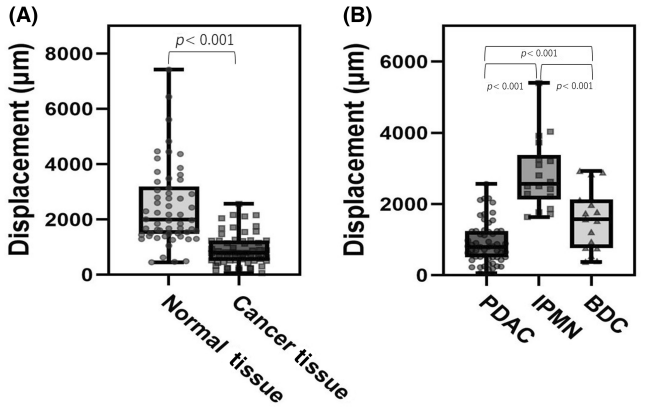


**FIGURE 2** Results of the estimated stiffness of pancreatic and bile duct cancers. (A) Comparison between normal tissues and cancer tissues. (B) Comparison of histologic differences. BDC, bile duct cancer; IPMN, intraductal papillary mucinous neoplasm; PDAC, pancreatic ductal adenocarcinoma.

The ratio of positive areas of Azan-positive and αSMA-positive stroma, which are common markers for collagen fibers[18] and myofibroblasts, including cancer-associated fibroblasts,[19] tended to be greater in cases without preoperative therapy but were not statistically significant ($p=0.188$, $p=0.164$). The ratio of positive area of collagen I expression did not differ between the patients with and without preoperative therapy ($p=0.455$; Table 2).

Correlations between tumor stiffness and stromal components were examined in patients with PDAC. In patients without preoperative therapy, the displacement was negatively correlated with the ratio of the Azan-positive area ($\rho=-0.629$, $p=0.001$), αSMA area ($\rho=-0.812$, $p<0.001$), and collagen I area ($\rho=-0.59$, $p=0.003$). Displacement was not correlated with hyaluronic acid ($\rho=0.105$, $p=0.63$). A negative correlation between displacement and the ratio of Azan-positive ($\rho=-0.801$, $p<0.001$), αSMA-positive ($\rho=-0.878$, $p<0.001$), and collagen I-positive areas ($\rho=-0.653$, $p<0.001$) was also observed among patients who received preoperative therapy (Table 3). Thus, collagen fibers, collagen I, and αSMA$^+$ cancer-associated fibroblasts that produce and maintain the ECM, but not hyaluronic acid, contribute to tumor tissue stiffness. Although we also investigated the association between tumor stiffness and the clinicopathologic characteristics, including tumor necrosis, no differences in the clinical data and the presence of histological tumor necrosis were observed between soft versus hard tumors (Table S1).

### 3.4 | Association between tumor stiffness and immunological TME in PDAC

Heterogenic spatial distributions of the densities of tumor-infiltrating lymphocytes have been reported in PDAC. We segmented the tumor into the center and periphery for analysis of the immunological TME.[20] Representative multiplexed fluorescently labeled images and a representative slide segmented into the center and periphery are shown in Figure 4. To evaluate the relationship between stiffness and the immunological TME in PDAC with and without preoperative therapy, the median value of tumor displacement in cases without preoperative therapy (512.6 μm) was used as the cut-off value to divide cases into two groups: soft versus hard tumors. In the tumor center of PDAC in cases without preoperative therapy, the soft tumors had higher densities of immune cells, especially CD8$^+$ T cells and CD68$^+$/CD204$^+$ macrophages, compared to the hard tumors (Figure 5A). In the tumor periphery, although the density of CD68$^+$/CD204$^+$ macrophages was higher in soft tumors, the densities of both CD4$^+$ and CD8$^+$ T cells were comparable. These differences in the density of immune cells correlating with tumor stiffness were not observed in cases with preoperative therapy, either in the tumor center or periphery (Figure 5B). The density of CD3$^+$/CD8$^+$ T cells in the tumor center is higher in softer tumors. However, this relationship does not hold after preoperative therapy. Thus, preoperative treatments affected the association between tumor stiffness and immune cell densities.

### 3.5 | Association between stiffness and therapeutic effects

We hypothesized that the therapeutic antitumor effects might affect tumor stiffness in patients undergoing preoperative therapy. Therefore, we assessed the therapeutic effects by ART.[15,16] The median ART value was 112 mm$^2$ (range, 28.7–515.4 mm$^2$; Figure S3). The correlation between ART and pathological tumor size was moderate ($\rho=0.74$, $p<0.001$). No correlation was observed between ART and tumor stiffness ($\rho=0.074$, $p=0.67$; Figure 6). Thus, the efficacy of preoperative therapy did not seem to affect tumor stiffness.

### 3.6 | Tumor stiffness and early tumor recurrence

In patients with PDAC, the median follow-up duration was 21 months (interquartile range, 17–32 months). Early tumor recurrence was observed in 11 patients in the PDAC cohort. The incidence of early tumor recurrence was not different between the soft and hard groups (eight cases [19.0%] vs. three cases [18.7%]; $p=1.000$). Thus, tumor stiffness did not correlate with early tumor recurrence.

## 4 | DISCUSSION

In this study, we directly measured the displacement of PDAC after surgery and successfully examined the association between tumor stiffness and histological features. Our results suggest that tumor stiffness is influenced by tumor origin, pathology, and anticancer therapy, and is strongly associated with the histological features of the cancer stroma. Previously, we have reported an association between tumor stiffness and stroma in colon and pancreatic cancer using a tactile sensor, the Venustron system, in which we found strong associations

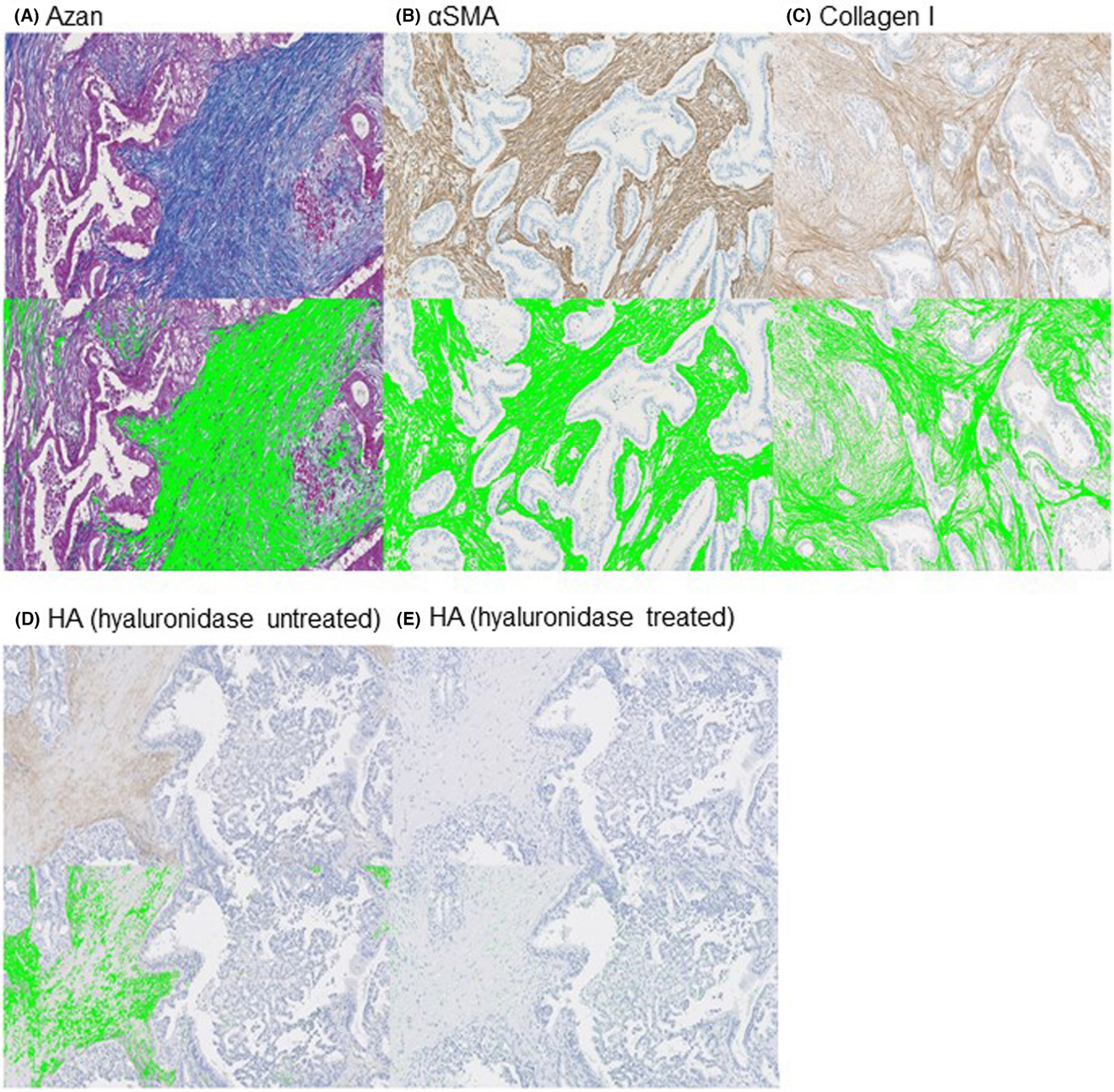


**FIGURE 3** Representative slides of pancreatic ductal adenocarcinoma tissue sections stained for (A) Azan–Mallory stain (Azan), (B) α-smooth muscle actin (αSMA), (C) collagen I, (D) hyaluronic acid (HA) without hyaluronidase treatment, and (E) HA with hyaluronidase treatment, and the morphometric analysis. Positively stained areas are identified as green in these images and calculated using morphometric software.

between tumor stiffness and Azan and αSMA positivity.[10,11] We tested the performance of the newly introduced tonometer iB-Dent using standard silicon samples, and consistent results were obtained using the Venustron system (Figure S1). In this study, strong associations between stiffness and Azan and αSMA positivity, but not hyaluronic acid, were also confirmed in PDAC, consistent with preclinical studies.[21] Other studies have reported that hyaluronic acid only plays a role in vessel compression in the presence of collagen.[22,23] In the current study, we analyzed and discovered the relationship between tumor stiffness and immunological TME in human cancer for the first time.

As tumor stiffness correlated with the biological and immunological TME, preoperative estimation of the stiffness might provide meaningful information regarding the indication for immune therapy. For example, the extracellular volume fraction, calculated from the unenhanced and equilibrium contrast-enhanced CT, has been reported to be a useful tool in estimating the degree of hepatic fibrosis.[24] Such data can be confirmed using our direct evaluation method.

One of the findings in this study was that PDAC treated with preoperative therapy was softer than that without preoperative therapy, suggesting that anticancer drugs not only influence tumor biology

but also tumor physics. We did not find any association between the alteration of tumor physics and the therapeutic effects of preoperative therapy, as estimated by ART, and early tumor recurrence. Thus, these results do not support the notion that tumor tissue stiffness is a biomarker of response to preoperative therapy in PDAC.

**TABLE 3** Correlation between pancreatic ductal adenocarcinoma stiffness and the ratio of Azan, α-smooth muscle actin (αSMA), hyaluronic acid, and collagen I

| | Stromal component | Spearman $\rho$[a] | *p* value |
|---|---|---|---|
| Without preoperative treatment ($n=23$) | Azan | −0.629 | 0.001 |
| | αSMA | −0.812 | <0.001 |
| | Hyaluronic acid | 0.105 | 0.630 |
| | Collagen I | −0.590 | 0.003 |
| With preoperative treatment ($n=35$) | Azan | −0.801 | <0.001 |
| | αSMA | −0.878 | <0.001 |
| | Hyaluronic acid | −0.060 | 0.740 |
| | Collagen I | −0.653 | <0.001 |

[a]$\rho$: 0–0.3, uncorrelated; 0.3–0.6, weakly correlated; 0.6–0.8, moderately correlated; >0.8, strongly correlated.

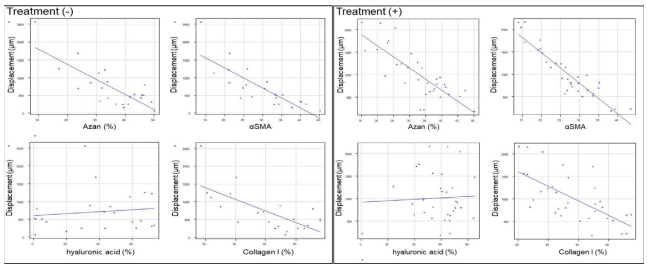


Preoperative therapy acts by killing proliferating cancer cells, which are softer than normal cells when measured using atomic force microscopy,[25] and to a lesser extent, proliferating cancer-associated fibroblasts, which produce and maintain the ECM. Accordingly, we observed that the fraction of the tumor area containing hyaluronic acid was enriched, as anticancer therapy reduced the density of cells. In addition, a slight but nonsignificant decrease in the ratio of Azan- and αSMA-positive areas in stromal tissues was found in this study. Given the correlation between stiffness and collagen,[26] stiffness of PDAC after preoperative therapy was nearly half of that without, in our study. Thus, we speculated that an alteration in tumor stiffness after therapy mainly depended on the biological alteration in stromal tissue rather than that in individual cancer cells. Furthermore, Ueno et al. morphologically classified the fibrous stroma of advanced rectal cancers into mature and immature stroma, based on the histologically identified stromal components. Immature stroma was associated with poor overall survival, more budding, and sparser T cells.[27] Such pathological assessment methods to classify cancer stroma could elucidate the association between tumor stroma and the stiffness.

Currently, preoperative therapy followed by radical surgery is the standard therapeutic strategy for resectable PDAC.[28] Furthermore, the antihypertensive drug losartan, repurposed to the preoperative setting in resectable PDAC, was shown to reduce cancer-associated fibroblast, collagen I, and hyaluronic acid levels.[22] Losartan increased the proportion of patients who underwent complete surgical resection for initially diagnosed locally advanced PDAC.[29] Based on these results, losartan is currently being investigated in combination with cytotoxic therapy in patients with PDAC (NCT03563248). Therefore, modulation of the physical properties of the TME in PDAC patients could lead to improved therapeutic outcomes.

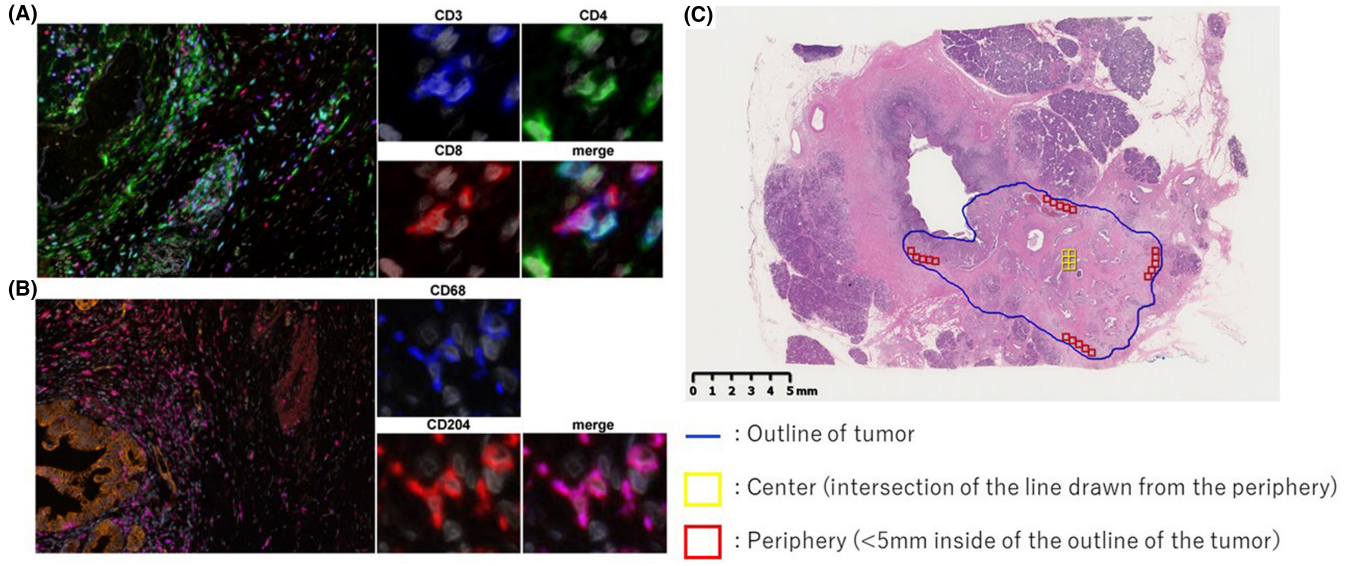


**FIGURE 4** Representative multiplexed fluorescently labeled images of pancreatic ductal adenocarcinoma. (A) Nuclei, gray; CD3, blue; CD4, green; CD8, red. (B) Nuclei, gray; cytokeratin, orange; CD68, blue; CD 204, red. (C) Representative slide segmented into the center and periphery.

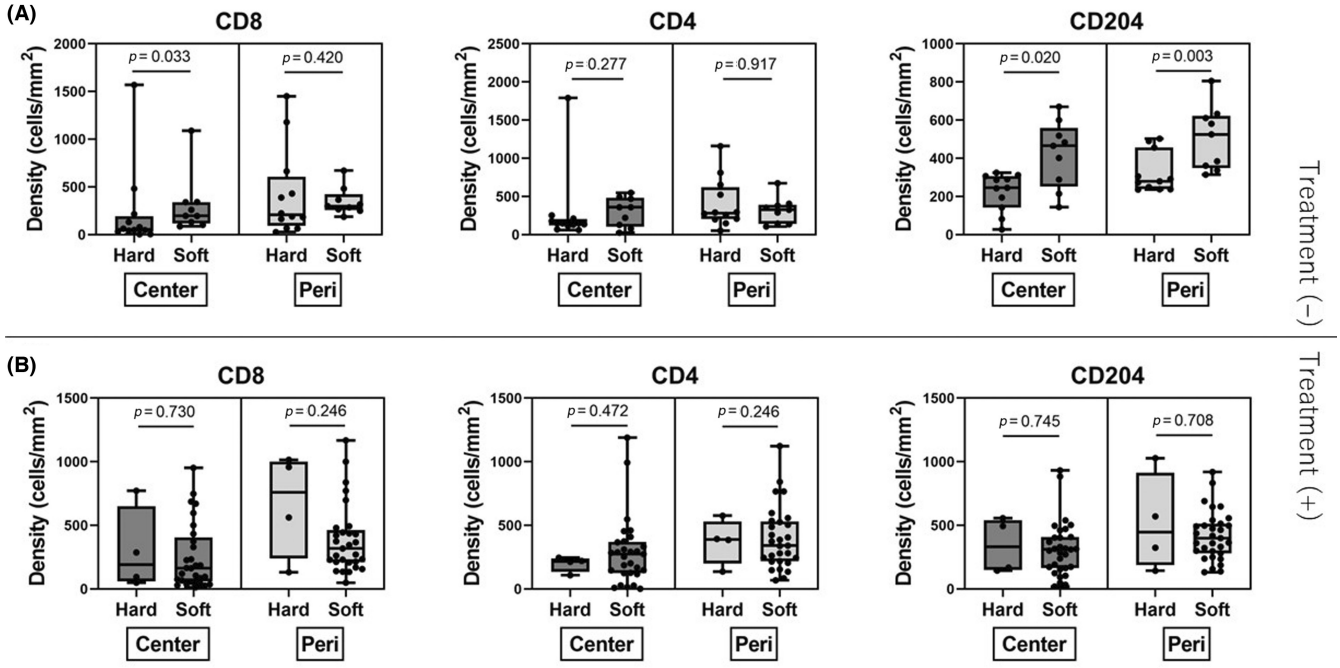


FIGURE 5 Analysis of stiffness and the immunological tumor microenvironment in the tumor center and periphery of pancreatic ductal adenocarcinomas. (A) Cases without preoperative therapy. Soft, 12 cases; hard, 11 cases. (B) Cases with preoperative therapy. Soft, 31 cases; hard, 4 cases.

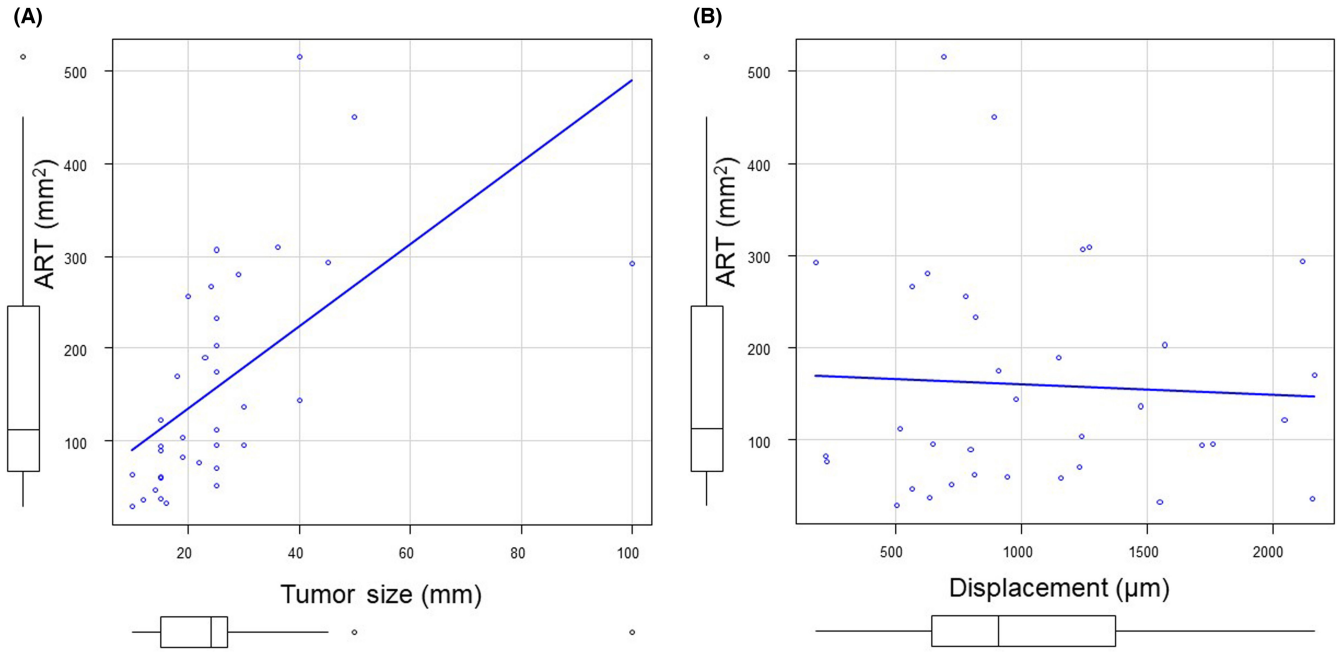


FIGURE 6 (A) Scatter plot shows moderate correlation between pancreatic ductal adenocarcinoma tumor size and area of residual tumor ($\rho = 0.74$, $p < 0.001$). (B) Scatter plot did not show significant correlations between tumor stiffness and residual tumor area ($\rho = 0.0737$, $p = 0.673$).

Immunotherapy has revolutionized the treatment of multiple advanced-stage malignancies. However, only a fraction of PDAC patients respond to novel immune checkpoint inhibitors, and the TME in PDAC compromises the efficacy of cancer therapy through limited drug delivery, providing mechanical barriers to exclude T cell trafficking into the tumor.[30,31] In this study, we observed for the first time in human cancer tissues that the physical TME showed correlations with the immunological TME. We found a lower accumulation of $CD3^+/CD8^+$ T cells and $CD68^+/CD204^+$ macrophages in the center of tumors in hard PDAC compared with soft PDAC. In pancreatic cancers, the fibrous stroma is hypothesized to serve as a mechanical barrier for various drugs.[32] The spatial heterogeneity of

the immunological TME observed in our study can be attributed to the mechanical barrier effect.

The present study had certain limitations. First, this was a single-center retrospective study within a relatively short observational period. Second, although the measurement of stiffness was carried out in a well-established manner, reproducibility is an important consideration. The surface of the pancreas is not completely flat, and the physical characteristics that are not reflected in histologic features might create marked variability in the data between cases. Third, as we selected one representative slide for the analysis of multiplexed fluorescent immunohistochemistry, the analysis might not have captured the heterogeneity in large tumors that exceeded two or more slides. A multicenter study with a larger number of cases is warranted.

To conclude, we compared tumor stiffness and pathological features and observed the relationship between the physical and immunological TME in human PDAC. Preoperative therapy could alter the physical and immunological TME. Further understanding of the TME in both physical and immunological aspects could lead to the development of novel therapeutic strategies.

## AUTHOR CONTRIBUTIONS

Study concept and design: all authors. Acquisition of data: YI, MK, Toshiyuki S, RM, and Toshihiro S. Analysis and interpretation of data: YI, MK, Toshiyuki S, GI, Toshihiro S, JDM, Triantafyllos S and HC. Drafting of the manuscript: YI, MK and Toshihiro S. Critical revision of the manuscript for intellectual context: all authors. Final approval of the of the manuscript for publication: all authors. Accountable for all aspects of the work: all authors.

## ACKNOWLEDGMENTS

The authors thank Yuka Nakamura (Division of Pathology, Exploratory Oncology Research and Clinical Trial Center, National Cancer Center) for technical assistance. We would like to thank Editage for English language editing.

## FUNDING INFORMATION

This work was funded by the Fund for the Promotion of Joint International Research, Fostering Joint International Research (B), No. 21KK0197.

## CONFLICT OF INTEREST STATEMENT

John D. Martin is an employee of Red Arrow Therapeutics Co. Ltd. Genichiro Ishii is an editorial board member of *Cancer Science*. The other authors have no conflicts of interest to declare.

## DATA AVAILABILITY STATEMENT

The datasets used and analyzed during the current study are available from the corresponding author upon reasonable request.

## ETHICS STATEMENTS

Approval of the research protocol by an institutional review board: This study was approved by the institutional review board of the National Cancer Center (IRB number: 2012-067).

Informed consent: Informed consent was obtained from all participants involved in the study.

Registry and registration no. of the study/trial: N/A.

Animal studies: N/A.

## ORCID

*Yu Igata* https://orcid.org/0000-0001-5074-417X
*Motohiro Kojima* https://orcid.org/0000-0002-6150-6545
*Genichiro Ishii* https://orcid.org/0000-0001-8637-3323
*Masashi Kudo* https://orcid.org/0000-0003-2161-1807
*Shin Kobayashi* https://orcid.org/0000-0001-9321-8452

## REFERENCES

1. Edwards P, Kang BW, Chau I. Targeting the stroma in the management of pancreatic cancer. *Front Oncol*. 2021;11:691185.
2. Maneshi P, Mason J, Dongre M, Öhlund D. Targeting tumor-stromal interactions in pancreatic cancer: impact of collagens and mechanical traits. *Front Cell Dev Biol*. 2021;9:787485.
3. Schober M, Jesenofsky R, Faissner R, et al. Desmoplasia and chemoresistance in pancreatic cancer. *Cancers*. 2014;6:2137-2154.
4. Muller M, Haghnejad V, Schaefer M, et al. The immune landscape of human pancreatic ductal carcinoma: key players, clinical implications, and challenges. *Cancers*. 2022;14:995.
5. Martin JD, Fukumura D, Duda DG, Boucher Y, Jain RK. Reengineering the tumor microenvironment to alleviate hypoxia and overcome cancer heterogeneity. *Cold Spring Harb Perspect Med*. 2016;6:a027094.
6. Nia HT, Munn LL, Jain RK. Physical traits of cancer. *Science*. 2020;370:eaaz0868.
7. Stylianopoulos T, Martin JD, Chauhan VP, et al. Causes, consequences, and remedies for growth-induced solid stress in murine and human tumors. *Proc Natl Acad Sci U S A*. 2012;109:15101-15108.
8. Jain RK. Normalizing tumor microenvironment to treat cancer: bench to bedside to biomarkers. *J Clin Oncol*. 2013;31:2205-2218.
9. Stylianopoulos T, Munn LL, Jain RK. Reengineering the physical microenvironment of tumors to improve drug delivery and efficacy: from mathematical modeling to bench to bedside. *Trends Cancer*. 2018;4:292-319.
10. Kawano S, Kojima M, Higuchi Y, et al. Assessment of elasticity of colorectal cancer tissue, clinical utility, pathological and phenotypical relevance. *Cancer Sci*. 2015;106:1232-1239.
11. Sugimoto M, Takahashi S, Kojima M, et al. What is the nature of pancreatic consistency? Assessment of the elastic modulus of the pancreas and comparison with tactile sensation, histology, and occurrence of postoperative pancreatic fistula after pancreaticoduodenectomy. *Surgery*. 2014;156:1204-1211.
12. Kudo M, Ishii G, Gotohda N, et al. Histological tumor necrosis in pancreatic cancer after neoadjuvant therapy. *Oncol Rep*. 2022;48:121.
13. Takahashi D, Kojima M, Suzuki T, et al. Profiling the tumour immune microenvironment in pancreatic neuroendocrine neoplasms with multispectral imaging indicates distinct subpopulation characteristics concordant with WHO 2017 classification. *Sci Rep*. 2018;8:13166.
14. Morisue R, Kojima M, Suzuki T, et al. Sarcomatoid hepatocellular carcinoma is distinct from ordinary hepatocellular carcinoma: clinicopathologic, transcriptomic and immunologic analyses. *Int J Cancer*. 2021;149:546-560.
15. Matsuda Y, Ohkubo S, Nakano-Narusawa Y, et al. Objective assessment of tumor regression in post-neoadjuvant therapy resections for pancreatic ductal adenocarcinoma: comparison of multiple tumor regression grading systems. *Sci Rep*. 2020;10:18278.

16. Okubo S, Kojima M, Matsuda Y, et al. Area of residual tumor (ART) can predict prognosis after post neoadjuvant therapy resection for pancreatic ductal adenocarcinoma. *Sci Rep*. 2019;9:17145.
17. Kanda Y. Investigation of the freely available easy-to-use software 'EZR' for medical statistics. *Bone Marrow Transplant*. 2013;48:452-458.
18. Mallory FB. A contribution to staining methods: I. A differential stain for connective-tissue fibtillae and reticulum. II. Chloride of iron haematoxylin for nuclei and fibrin. III. Phosphotungstic acid haematoxylin for neuroglia fibres. *J Exp Med*. 1900;5:15-20.
19. Nurmik M, Ullmann P, Rodriguez F, Haan S, Letellier E. In search of definitions: cancer-associated fibroblasts and their markers. *Int J Cancer*. 2020;146:895-905.
20. Masugi Y, Abe T, Ueno A, et al. Characterization of spatial distribution of tumor-infiltrating CD8(+) T cells refines their prognostic utility for pancreatic cancer survival. *Mod Pathol*. 2019;32:1495-1507.
21. Roose T, Netti PA, Munn LL, Boucher Y, Jain RK. Solid stress generated by spheroid growth estimated using a linear poroelasticity model. *Microvasc Res*. 2003;66:204-212.
22. Chauhan VP, Martin JD, Liu H, et al. Angiotensin inhibition enhances drug delivery and potentiates chemotherapy by decompressing tumour blood vessels. *Nat Commun*. 2013;4:2516.
23. Voutouri C, Polydorou C, Papageorgis P, Gkretsi V, Stylianopoulos T. Hyaluronan-derived swelling of solid tumors, the contribution of collagen and cancer cells, and implications for cancer therapy. *Neoplasia*. 2016;18:732-741.
24. Shinagawa Y, Sakamoto K, Sato K, Ito E, Urakawa H, Yoshimitsu K. Usefulness of new subtraction algorithm in estimating degree of liver fibrosis by calculating extracellular volume fraction obtained from routine liver CT protocol equilibrium phase data: preliminary experience. *Eur Radiol*. 2018;103:99-104.
25. Guo X, Bonin K, Scarpinato K, Guthold M. The effect of neighboring cells on the stiffness of cancerous and non-cancerous human mammary epithelial cells. *New J Phys*. 2014;16:105002.
26. Netti PA, Berk DA, Swartz MA, Grodzinsky AJ, Jain RK. Role of extracellular matrix assembly in interstitial transport in solid tumors. *Cancer Res*. 2000;60:2497-2503.
27. Ueno H, Jones AM, Wilkinson KH, Jass JR, Talbot IC. Histological categorisation of fibrotic cancer stroma in advanced rectal cancer. *Gut*. 2004;53:581-586.
28. National Comprehensive Cancer Network. Pancreatic Cancer (Version 1.2022). Accessed: 26 May 2022. Available from: https://www.nccn.org/professionals/physician_gls/pdf/pancreatic.pdf
29. Murphy JE, Wo JY, Ryan DP, et al. Total neoadjuvant therapy with FOLFIRINOX in combination with losartan followed by chemoradiotherapy for locally advanced pancreatic cancer: a Phase 2 clinical trial. *JAMA Oncol*. 2019;5:1020-1027.
30. Huber M, Brehm CU, Gress TM, et al. The immune microenvironment in pancreatic cancer. *Int J Mol Sci*. 2020;21:7307.
31. Olive KP, Jacobetz MA, Davidson CJ, et al. Inhibition of Hedgehog signaling enhances delivery of chemotherapy in a mouse model of pancreatic cancer. *Science*. 2009;324:1457-1461.
32. Tanaka HY, Kano MR. Stromal barriers to nanomedicine penetration in the pancreatic tumor microenvironment. *Cancer Sci*. 2018;109:2085-2092.

## SUPPORTING INFORMATION

Additional supporting information can be found online in the Supporting Information section at the end of this article.

**How to cite this article:** Igata Y, Kojima M, Suzuki T, et al. Relationships between physical and immunological tumor microenvironment in pancreatic ductal adenocarcinoma. *Cancer Sci*. 2023;114:3783-3792. doi:10.1111/cas.15853